On the non-uniqueness of the electromagnetic instantaneous response

2003 J. Phys. A: Math. Gen. 36 1743

(http://iopscience.iop.org/0305-4470/36/6/317)

INSTITUTE OF PHYSICS PUBLISHING JOURNAL OF PHYSICS A: MATHEMATICAL AND GENERAL

J. Phys. A: Math. Gen. **36** (2003) 1743–1758 PII: S0305-4470(03)54227-5

On the non-uniqueness of the electromagnetic instantaneous response

Mats Gustafsson

Department of Electroscience, Electromagnetic Theory, Lund Institute of Technology, Lund University, Box 118 S-221 00 Lund, Sweden

E-mail: mats@es.lth.se

Received 1 October 2002
Published 29 January 2003
Online at stacks.iop.org/JPhysA/36/1743

Abstract

The instantaneous response models the rapid part of the interaction between electromagnetic fields and materials. From a physical point of view the instantaneous response is non-observable and from a mathematical point of view it constitutes the principal part of the Maxwell equations. In this paper, it is shown that the instantaneous response is not uniquely determined from a given set of values of the constitutive map. The given values only give an upper bound on the size of the instantaneous response. A numerical example illustrates the non-uniqueness of the instantaneous response.

PACS numbers: 03.50.De, 02.30.Zz, 02.60.Lj

1. Introduction

Electromagnetic interaction with material is diverse. It ranges from the linear, isotropic and non-dispersive interaction with diluted gases to the highly nonlinear behaviour of iron. The material interacts with the electromagnetic field through the dynamics of the microscopic charges of the material, i.e. the charges of the atoms and the molecules. At a macroscopic level, the electromagnetic interaction with material is modelled by constitutive relations. The constitutive relations are based on a continuum model of the material, i.e. the interaction at a microscopic level is replaced by a set of effective material parameters [9, 20, 25]. The spatial distribution of the microscopic charges and the dynamics of the microscopic charges offer phenomena such as direction dependence and memory effects of the constitutive relations [9, 20, 21].

The mathematical models of the interaction have been thoroughly investigated, see, e.g., [5, 8, 14, 20, 23, 25, 27, 33] for a general discussion about electromagnetic modelling. In [9, 28], the connection between the microscopic Maxwell equations and the macroscopic Maxwell equations is analysed, see also [22]. General time-domain constitutive relations are given in [21], see also [15]. Optical and magnetic properties are, e.g., discussed in [6] and [7],

respectively. An analysis of the interaction between electromagnetic and elastodynamic properties is given in [11, 12].

The constitutive relations of a material are determined either from direct measurements or from *a priori* knowledge of the microscopic structure of the material. In general, this offers an accurate description of the interaction in a specific frequency and amplitude range. The set of constitutive relations can be used for an electromagnetic application as long as the fields of the application are restricted to the same frequency and amplitude range. In time-domain formulations, e.g., FDTD, it is necessary to extend the definition of the constitutive relations to all frequencies. The constitutive relations can be extended outside their range of validity as long as the solubility of the Maxwell equations is not affected, see also figure 2.

The instantaneous (or high-frequency or optical) response models the rapid part of the interaction between electromagnetic fields and materials. It is given by the high-frequency asymptote of the Laplace-domain constitutive map or equivalently as the small time approximation of the time-domain constitutive map. From a mathematical as well as a computational point of view, the instantaneous response is of considerable importance. Together with the curl operators it constitutes the principal part of the Maxwell equations and hence controls many of the mathematical properties of the solution, e.g., existence, uniqueness and continuity [13, 24]. The instantaneous response is also of considerable importance in numerical approximations, e.g., in stability conditions of finite difference schemes (FDTD) [31, 32], see also [30], where computational errors due to an erroneous instantaneous response for pulse propagation in a dispersive slab are analysed. Due to the theoretical as well as the practical importance of the instantaneous response, it is vital to study the uniqueness of the instantaneous response, i.e. how the instantaneous response is determined by the values of the constitutive map.

In this paper, a set of constitutive relations is constructed to show that the instantaneous response is non-unique. Moreover, Nevanlinna–Pick theory [1, 10] is used to show that the given values of the constitutive relations only give an upper bound on the size of the instantaneous response [30].

To start, it is conjecture that the instantaneous response is undetermined from a physical point of view, i.e. it is not possible to measure the instantaneous response of the material. The non-observability of the instantaneous response follows from the break down of the macroscopic Maxwell equations for sufficiently high frequencies, i.e. the continuum model of a material is only accurate up to a specific frequency, typically somewhere between visual light and x-rays [20]. Above this frequency the macroscopic Maxwell equations do not give an accurate description of electromagnetic phenomena. At a microscopic level, the electromagnetic interaction is much more accurately modelled with theories such as quantum electrodynamics [34]. It is hence necessary to define the instantaneous response by extrapolation from the range of validity of the constitutive relations. However, physical arguments can be used to argue that the instantaneous response approaches its vacuum value for very high frequencies [25]. Moreover, the special theory of relativity states that the speed of electromagnetic waves in any medium cannot exceed the vacuum speed [20]. This predicts that it should always be possible to let the instantaneous response reduce to the vacuum value.

In typical engineering applications of electromagnetics the instantaneous response is not restricted to the material properties at very high frequencies. The instantaneous response is instead determined by extrapolation from the values of the constitutive relations in the frequency band of the application, see also figure 1.

It is well known that the constitutive map is analytic [2] and it is also well known that an analytic function is determined from its values in a neighbourhood of a point [2, 17]. Hence, in principle, the instantaneous response is determined from the low-frequency values of the

constitutive map. However, this analytical continuation is ill-posed, i.e. small errors of the constitutive map can give large errors of the instantaneous response.

The outline of this paper is as follows. In section 2, the Maxwell equations, the notation and some basic properties of the constitutive map are introduced. The extension of the constitutive map to the time domain from the frequency domain is discussed in section 3. An explicit construction to show the non-uniqueness of the instantaneous response is given in section 4. Nevanlinna–Pick theory is used in section 5 to give an upper bound on the size of the instantaneous response. In section 6, a numerical example is used to illustrate the non-uniqueness of the instantaneous response. In section 7 some conclusions are given.

2. The Maxwell equations and constitutive relations

The electromagnetic phenomena are described by the electric and magnetic fields, i.e. the electric field intensity $\boldsymbol{E}$, the magnetic field intensity $\boldsymbol{H}$, the electric flux density $\boldsymbol{D}$ and the magnetic flux density $\boldsymbol{B}$. The electromagnetic fields originate from the (electric) current density $\boldsymbol{J}$ and the charge density ϱ. In many problems it is convenient to include a magnetic current [4]. The electromagnetic fields are related through the Maxwell equations. The constitutive relations in this paper are general bi-anisotropic. For the analysis of wave propagation in these materials it is natural to use a six-vector formalism [19, 26]. The field intensities, flux densities and current densities are

$$\boldsymbol{e} = \begin{pmatrix} \epsilon_0^{1/2}\boldsymbol{E} \\ \mu_0^{1/2}\boldsymbol{H} \end{pmatrix} \qquad \boldsymbol{d} = \begin{pmatrix} \epsilon_0^{-1/2}\boldsymbol{D} \\ \mu_0^{-1/2}\boldsymbol{B} \end{pmatrix} \qquad \text{and} \qquad \boldsymbol{j} = \begin{pmatrix} \mu_0^{1/2}\boldsymbol{J} \\ \boldsymbol{0} \end{pmatrix} \tag{2.1}$$

respectively. Observe that the electromagnetic fields in (2.1) are scaled by the free-space permittivity, ϵ_0, and the free-space permeability, μ_0, such that the field intensities and flux densities have the unit (energy/volume)$^{1/2}$. With this notation, the Maxwell equations are written as

$$\partial_t \boldsymbol{d} - \nabla \times \mathrm{J}\boldsymbol{e} = -\boldsymbol{j} \qquad \text{where} \quad \mathrm{J} = \begin{pmatrix} 0 & 1 \\ -1 & 0 \end{pmatrix}. \tag{2.2}$$

The geometrical and the field structure of the (combined) field intensity are distinguished by the use of vector notation, e.g., the scalar product $\boldsymbol{E}\cdot$ and the vector product $\boldsymbol{E}\times$, for the geometrical part and matrix notation, e.g., the transpose $\boldsymbol{e}^{\mathrm{T}}$ and the Hermitean transpose $\boldsymbol{e}^{\mathrm{H}}$, for the field part. As an example, the squared absolute value of the field intensity is

$$\begin{aligned} |\boldsymbol{e}|^2 = \boldsymbol{e}^{\mathrm{H}} \cdot \boldsymbol{e} &= \begin{pmatrix} \epsilon_0^{1/2}\boldsymbol{E}^* & \mu_0^{1/2}\boldsymbol{H}^* \end{pmatrix} \cdot \begin{pmatrix} \epsilon_0^{1/2}\boldsymbol{E} \\ \mu_0^{1/2}\boldsymbol{H} \end{pmatrix} \\ &= \epsilon_0 \boldsymbol{E}^* \cdot \boldsymbol{E} + \mu_0 \boldsymbol{H}^* \cdot \boldsymbol{H} = \epsilon_0 |\boldsymbol{E}|^2 + \mu_0 |\boldsymbol{H}|^2 \end{aligned} \tag{2.3}$$

where $*$ denotes the complex conjugate, see [19] for details about this notation.

The Laplace domain is frequently used in the analysis. The Laplace transformed wave-field quantities are denoted with a hat, i.e.

$$\hat{\boldsymbol{e}}(\boldsymbol{x}, s) = \int_{0-}^{\infty} \mathrm{e}^{-st} \boldsymbol{e}(\boldsymbol{x}, t)\, \mathrm{d}t \qquad \text{and} \qquad \boldsymbol{e}(\boldsymbol{x}, t) = \frac{1}{2\pi} \int_{-\infty}^{\infty} \mathrm{e}^{(\eta + \mathrm{i}\omega)t} \hat{\boldsymbol{e}}(\boldsymbol{x}, \eta + \mathrm{i}\omega)\, \mathrm{d}\omega \tag{2.4}$$

where the Laplace transform parameter s is restricted to a right half plane defined by $s = \eta + \mathrm{i}\omega$ with $\eta \geqslant 0$. Before we can transform the Maxwell equations to the Laplace domain, the history ($\boldsymbol{e}(\boldsymbol{x}, t)$ for $t < 0$) of the field has to be removed. The history part is reinterpreted and included as a current term in the Maxwell equations. The assumptions for a linear dispersion law are: causal, spatially pointwise, continuous, linear and time invariant [8, 11, 12, 21].

A map $\boldsymbol{e} \to \boldsymbol{d}$ satisfying the above requirements has a representation in the form of a temporal convolution. In the Laplace domain, the convolution corresponds to the well-known matrix representation

$$\hat{\boldsymbol{d}}(\boldsymbol{x}, s) = \varepsilon(\boldsymbol{x}, s)\hat{\boldsymbol{e}}(\boldsymbol{x}, s) \tag{2.5}$$

where ε is a 2×2 matrix with complex-valued dyadic entries. Causality is guaranteed by the requirement that the elements of $\varepsilon(\boldsymbol{x}, x)$ are analytic functions of s for $\operatorname{Re} s > \eta_0$ for some $\eta_0 > -\infty$. Furthermore, the matrix elements are real valued if the Laplace parameter is real valued. The Maxwell equations are written as

$$s\varepsilon(\boldsymbol{x}, s)\hat{\boldsymbol{e}} - \nabla \times \mathrm{J}\hat{\boldsymbol{e}} = -\hat{\boldsymbol{\jmath}}(\boldsymbol{x}, s) \tag{2.6}$$

in the Laplace domain.

A material is passive if the material does not produce energy. From the Poynting theorem [8, 14, 20, 25], we get the following sufficient condition for passivity. The constitutive map ε is passive if [19]

$$\operatorname{Re} s\varepsilon(\boldsymbol{x}, s) \geqslant 0 \qquad \text{for} \quad s \in \mathbb{C}_+ = \{s = \eta + \mathrm{i}\omega : \eta > 0, \omega \in \mathbb{R}\}. \tag{2.7}$$

This inequality is a shorthand notation for a non-negative definite symmetric part of the constitutive map, i.e. $\operatorname{Re}\{\boldsymbol{u}^{\mathrm{H}} \cdot s\varepsilon(\boldsymbol{x}, s)\boldsymbol{u}\} \geqslant 0$ for all $\boldsymbol{u} \in \mathbb{C}^3 \times \mathbb{C}^3$ and $s \in \mathbb{C}_+$. Passivity (2.7) enters as a natural restriction for most materials, i.e. the given values of the constitutive map are assumed to satisfy (2.7). In the problem to extend the definition of the constitutive map to the time domain, the passivity (2.7) enters as a stability requirement. The passivity ensures that the time-domain solution does not grow too fast as time evolves, i.e. errors that are introduced by the extrapolation of the constitutive map remains sufficiently small.

The constitutive relations are decomposed into an instantaneously reacting part and a non-instantaneous part. The instantaneous (or optical, or high-frequency) response models the rapid part of the interaction between the electromagnetic fields and the material. In the Laplace domain, the instantaneous response corresponds to the high-frequency behaviour, i.e.

$$\varepsilon(\boldsymbol{x}, s) = \varepsilon_\infty(\boldsymbol{x}) + \mathrm{O}(s^{-1}) \qquad \text{as} \quad \mathbb{C}_+ \ni s \to \infty. \tag{2.8}$$

Observe that the passivity implies that the instantaneous response is symmetric positive semidefinite, i.e. $\operatorname{Im}\varepsilon_\infty = 0$ and $\varepsilon_\infty \geqslant 0$, see [15, 19]. Here, $\operatorname{Im}\varepsilon_\infty = 0$ is a shorthand notation for $\operatorname{Im}\{\boldsymbol{u}^{\mathrm{H}} \cdot \varepsilon_\infty \boldsymbol{u}\} = 0$ for all $\boldsymbol{u} \in \mathbb{C}^3 \times \mathbb{C}^3$. To ensure a well-posed form of the Maxwell equations, the instantaneous response is assumed to be symmetric positive definite, i.e.

$$\operatorname{Im}\varepsilon_\infty = 0 \qquad \text{and} \qquad \varepsilon_\infty \geqslant \varepsilon_{\mathrm{inf}} > 0 \tag{2.9}$$

for some positive constant $\varepsilon_{\mathrm{inf}}$.

The passivity is used in the convergence proof of the approximate constitutive relations in section 4.2. The estimates are based on the following inequality. Let $\varepsilon(s)$ be a passive constitutive map with the Hermitean instantaneous response ε_∞, i.e. (2.7), (2.8) and (2.9). Then the symmetric part of $s\varepsilon$ is bounded from below by the symmetric part of $s\varepsilon_\infty$, i.e.

$$\operatorname{Re}\{s\varepsilon(s)\} \geqslant \varepsilon_\infty \operatorname{Re} s \qquad \text{for all } s \in \mathbb{C}_+ \tag{2.10}$$

or equivalently $\operatorname{Re}\{\boldsymbol{u}^{\mathrm{H}} \cdot s\varepsilon(s)\boldsymbol{u}\} \geqslant \boldsymbol{u}^{\mathrm{H}} \cdot \varepsilon_\infty \boldsymbol{u} \operatorname{Re} s$ for all $\boldsymbol{u} \in \mathbb{C}^3 \times \mathbb{C}^3$ and $s \in \mathbb{C}_+$. To show this estimate the identity $\operatorname{Re}\{s\varepsilon(s)\} = \operatorname{Re}\{s(\varepsilon(s) - \varepsilon_\infty)\} + \operatorname{Re}\{s\varepsilon_\infty\}$ is used. The first term on the right-hand side is estimated by the minimum principle for harmonic functions [2, 17] together with the fact that the real-valued part of the high-frequency response vanishes at the boundary, i.e. $\operatorname{Re}\{\mathrm{i}\omega\varepsilon_\infty\} = 0$ since $\operatorname{Im}\varepsilon_\infty = 0$. This gives

$$\operatorname{Re}\{s(\varepsilon(s) - \varepsilon_\infty)\} \geqslant \inf_{\omega\in\mathbb{R}} \operatorname{Re}\{\mathrm{i}\omega(\varepsilon(\mathrm{i}\omega) - \varepsilon_\infty)\} = \inf_{\omega\in\mathbb{R}} \operatorname{Re}\{\mathrm{i}\omega\varepsilon(\mathrm{i}\omega)\} = 0 \tag{2.11}$$

for all $s \in \mathbb{C}_+$. The estimate (2.10) follows from $\operatorname{Re}\{s\varepsilon_\infty\} = \varepsilon_\infty \operatorname{Re} s$ for all symmetric ε_∞ together with (2.11).

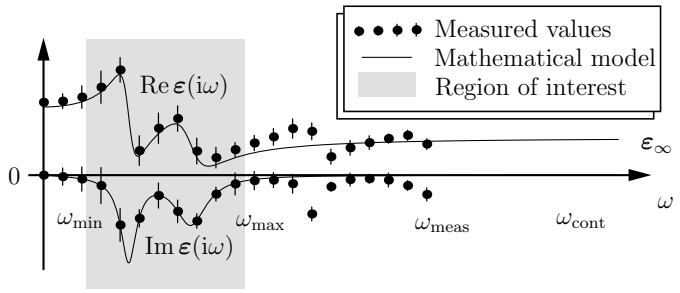

Figure 1. Illustration of the range of validity of the constitutive relations. The measured values of the constitutive map ε are given up to frequency ω_{meas}, the mathematical model is used for frequencies in the interval $[\omega_{\min}, \omega_{\max}]$, and ω_{cont} is the upper limit for the use of a continuum model of the medium.

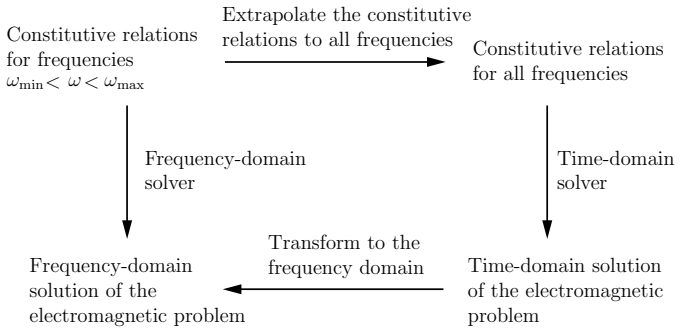

Figure 2. An electromagnetic problem can either be solved in the frequency domain or in the time domain. In the time-domain solution, the definitions of the constitutive relations are first extended to all frequencies, or equivalently to the time domain. A time-domain algorithm followed by an inverse Fourier transform gives the desired frequency-domain solution of the original problem. In this paper, we study how the constitutive relations can be extrapolated such that the time-domain approach can be used to give the frequency-domain solution.

3. Frequency and time-domain data

In this paper, we consider an electromagnetic problem in the frequency range $[\omega_{\min}, \omega_{\max}]$. The values of the constitutive map are given in the same frequency range, i.e.

$$\varepsilon(\mathrm{i}\omega) \qquad \text{for} \quad \omega \in [\omega_{\min}, \omega_{\max}] \tag{3.1}$$

are provided, see figure 1. The electromagnetic problem can either be solved in the frequency domain or in the time domain, see figure 2. In the frequency-domain solution, it is sufficient to use the values of ε in the given frequency range. However, in the time-domain approach it is necessary to extend the definition of ε to all frequencies, i.e. the time-domain map $\boldsymbol{d} = \varepsilon[\boldsymbol{e}]$. Here, we study how the map $\varepsilon(\mathrm{i}\omega)$ can be continued outside the frequency range $[\omega_{\min}, \omega_{\max}]$. In this paper we focus on the high-frequency value of ε, i.e.

$$\varepsilon_\infty = \lim_{\omega \to \infty} \varepsilon(\mathrm{i}\omega). \tag{3.2}$$

The basic assumptions of the linear dispersion law above are not sufficient to give a well-defined extension of the constitutive map. The assumption of passivity and a positive definite instantaneous response are used to get a well-defined extension of the constitutive map.

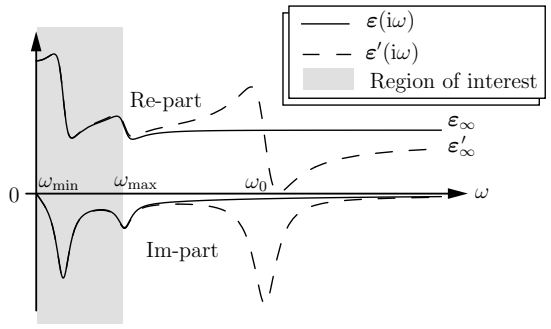

Figure 3. Illustration of the approximation of the constitutive relations. The original constitutive map $\varepsilon(\mathrm{i}\omega)$ with the instantaneous response ε_∞ is approximated by the constitutive map $\varepsilon'(\mathrm{i}\omega)$ with the instantaneous response $\varepsilon'_\infty < \varepsilon_\infty$. The error of the approximation approaches zero in the region of interest $[0, \omega_{\max}]$ as the approximation parameter $\omega_0 \to \infty$.

4. Non-uniqueness of the instantaneous response

By an explicit construction below, it is shown that the instantaneous response is non-unique. Let the original constitutive relations be given by a bi-anisotropic model with an instantaneous response ε_∞. This model is assumed to be accurate in the frequency range $[\omega_{\min}, \omega_{\max}]$. The goal is to construct an approximate set of constitutive relations that have the high-frequency response $\varepsilon'_\infty < \varepsilon_\infty$ and give good approximations of the original fields, see figure 2.

In section 4.1, an approximate model ε' is constructed such that the error of $\varepsilon'(\mathrm{i}\omega)$ is small in the frequency range $[\omega_{\min}, \omega_{\max}]$. In section 4.2, the error of the fields associated with the ε' are shown to be small in both the time and frequency domains.

4.1. Operator approximation

In this section an approximate set of constitutive relations, ε', is constructed such that the material model agrees well with the original one in the frequency range $[\omega_{\min}, \omega_{\max}]$ and that the high-frequency response is $\varepsilon'_\infty < \varepsilon_\infty$. An admissible approximate constitutive map ε' is given by

$$\varepsilon'(s) = \varepsilon(s) + \left(\frac{\omega_0^2}{s^2 + \nu s + \omega_0^2} - 1 \right) (\varepsilon_\infty - \varepsilon'_\infty) \tag{4.1}$$

where ε'_∞ is the new high-frequency response and $\nu \geqslant 0$ and ω_0 are model parameters, see figure 3. Observe that this is a mathematical construction, i.e. it is not required that the values of $\varepsilon'(\mathrm{i}\omega)$ correspond to an actual material outside the interval $[\omega_{\min}, \omega_{\max}]$. The model is passive if $0 < \varepsilon'_\infty < \varepsilon_\infty$, i.e.

$$\operatorname{Re} s\varepsilon' \geqslant \operatorname{Re} \left\{ s\varepsilon'_\infty + \frac{s\omega_0^2}{s^2 + \nu s + \omega_0^2} (\varepsilon_\infty - \varepsilon'_\infty) \right\} \geqslant \varepsilon'_\infty \operatorname{Re} s \tag{4.2}$$

where we have used the inequality (2.10) based on the analytic properties of passive constitutive maps. The 'error' in the approximation is

$$\begin{aligned} \sup_{\omega \in [\omega_{\min}, \omega_{\max}]} |\varepsilon'(\mathrm{i}\omega) - \varepsilon(\mathrm{i}\omega)| &= \sup_{\omega \in [\omega_{\min}, \omega_{\max}]} \left| \frac{-\omega^2 + \mathrm{i}\nu\omega}{-\omega^2 + \mathrm{i}\nu\omega + \omega_0^2} \right| \sup_{\boldsymbol{x} \in \mathbb{R}^3} |\varepsilon'_\infty - \varepsilon_\infty| \\ &\leqslant \frac{\omega_{\max}^2 + \nu\omega_{\max}}{\omega_0^2 - \omega_{\max}^2} \sup_{\boldsymbol{x} \in \mathbb{R}^3} |\varepsilon'_\infty - \varepsilon_\infty| \to 0 \qquad \text{as} \quad \omega_0 \to \infty \end{aligned} \tag{4.3}$$

where $|\varepsilon| = \sup_{|\boldsymbol{u}|=1} |\boldsymbol{u}^{\mathrm{H}} \cdot \varepsilon \boldsymbol{u}|$.

In the next section, we show that the approximation (4.1) also is sufficient to get good approximations of the solution of the Maxwell equations.

4.2. Convergence estimates

The approximation (4.1) is only meaningful if the fields $\boldsymbol{e}'$ associated with the approximate constitutive map ε' constitute a good approximation of the set of fields $\boldsymbol{e}$ associated with the original constitutive map ε. For notational simplicity, we consider an electromagnetic problem in $\mathbb{R}^3$ with quiescent initial fields, i.e. $\boldsymbol{e}(\boldsymbol{x}, t) = 0$ for $t \leqslant 0$. The current is assumed to be compactly supported and square integrable. Moreover, it is convenient to let the medium reduce to free space outside a sufficiently large sphere. Observe that this last requirement is no real restriction since we are only interested in time-domain results for fixed times, i.e. $0 \leqslant t \leqslant T$.

The original fields $\boldsymbol{e}(\boldsymbol{x}, t)$ solve the Maxwell equations

$$\partial_t \varepsilon[\boldsymbol{e}] - \nabla \times \mathrm{J}\boldsymbol{e} = -\boldsymbol{j}(\boldsymbol{x}, t) \qquad \text{for} \quad \boldsymbol{x} \in \mathbb{R}^3 \quad \text{and} \quad t \geqslant 0 \tag{4.4}$$

together with the initial conditions $\boldsymbol{e}(\boldsymbol{x}, t) = 0$ for $t \leqslant 0$. The corresponding approximate fields $\boldsymbol{e}'(\boldsymbol{x}, t)$ solve the Maxwell equations with the approximate constitutive map, i.e.

$$\partial_t \varepsilon'[\boldsymbol{e}'] - \nabla \times \mathrm{J}\boldsymbol{e}' = -\boldsymbol{j}(\boldsymbol{x}, t) \qquad \text{for} \quad \boldsymbol{x} \in \mathbb{R}^3 \quad \text{and} \quad t \geqslant 0 \tag{4.5}$$

together with the initial conditions $\boldsymbol{e}'(\boldsymbol{x}, t) = 0$ for $t \leqslant 0$. We are interested in the error of the approximate fields

$$\boldsymbol{e}'(\boldsymbol{x}, t) - \boldsymbol{e}(\boldsymbol{x}, t) \qquad \text{for} \quad \boldsymbol{x} \in \mathbb{R}^3 \quad \text{and} \quad 0 \leqslant t \leqslant T. \tag{4.6}$$

We use the Laplace-domain representation to get an error estimate of the approximate fields. Let $\hat{\boldsymbol{e}}(\boldsymbol{x}, s)$ be the solution of the Maxwell equations together with the constitutive map ε, i.e. $\hat{\boldsymbol{e}}$ solves

$$s\varepsilon(\boldsymbol{x}, s)\hat{\boldsymbol{e}} - \nabla \times \mathrm{J}\hat{\boldsymbol{e}} = -\hat{\boldsymbol{j}}(\boldsymbol{x}, s) \qquad \text{for} \quad \boldsymbol{x} \in \mathbb{R}^3 \tag{4.7}$$

together with the radiation conditions

$$\boldsymbol{x}/|\boldsymbol{x}| \times (\sqrt{\epsilon_0}\widehat{\boldsymbol{E}}(\boldsymbol{x}, s) + \boldsymbol{x}/|\boldsymbol{x}| \times \sqrt{\mu_0}\widehat{\boldsymbol{H}}(\boldsymbol{x}, s)) = \mathrm{o}(|\boldsymbol{x}|^{-1}) \qquad \text{as} \quad |\boldsymbol{x}| \to 0. \tag{4.8}$$

The approximate field satisfies

$$s\varepsilon'(\boldsymbol{x}, s)\hat{\boldsymbol{e}}' - \nabla \times \mathrm{J}\hat{\boldsymbol{e}}' = -\hat{\boldsymbol{j}}(\boldsymbol{x}, s) \qquad \text{for} \quad \boldsymbol{x} \in \mathbb{R}^3 \tag{4.9}$$

together with similar radiation conditions. The error $\hat{\boldsymbol{e}}' - \hat{\boldsymbol{e}}$ satisfies

$$s\varepsilon'(\boldsymbol{x}, s)(\hat{\boldsymbol{e}}' - \hat{\boldsymbol{e}}) - \nabla \times \mathrm{J}(\hat{\boldsymbol{e}}' - \hat{\boldsymbol{e}}) = -s(\varepsilon'(\boldsymbol{x}, s) - \varepsilon(\boldsymbol{x}, s))\hat{\boldsymbol{e}} \qquad \text{for} \quad \boldsymbol{x} \in \mathbb{R}^3. \tag{4.10}$$

We start with an energy estimate on the original fields (4.4). Multiply (4.7) from the left with $\hat{\boldsymbol{e}}^{\mathrm{H}}\cdot$ to get

$$s\hat{\boldsymbol{e}}^{\mathrm{H}} \cdot \varepsilon\hat{\boldsymbol{e}} - \hat{\boldsymbol{e}}^{\mathrm{H}} \cdot \nabla \times \mathrm{J}\hat{\boldsymbol{e}} = -\hat{\boldsymbol{e}}^{\mathrm{H}} \cdot \hat{\boldsymbol{j}}. \tag{4.11}$$

Integrate over $\mathbb{R}^3$ and estimate the terms. The first term is estimated with (2.10), i.e.

$$\operatorname{Re} s\hat{\boldsymbol{e}}^{\mathrm{H}} \cdot \varepsilon\hat{\boldsymbol{e}} \geqslant \eta\hat{\boldsymbol{e}}^{\mathrm{H}} \cdot \varepsilon_\infty\hat{\boldsymbol{e}} \geqslant \eta\varepsilon_{\inf}|\hat{\boldsymbol{e}}|^2 \tag{4.12}$$

where $\eta = \operatorname{Re} s$ is positive and $\varepsilon_{\inf} = \inf_{\boldsymbol{x}\in\mathbb{R}^3} \inf_{|\boldsymbol{u}|=1} \boldsymbol{u}^{\mathrm{H}} \cdot \varepsilon_\infty \boldsymbol{u}$. The second term vanishes due to the radiation condition and the third term is estimated with the Cauchy–Schwartz inequality, $\|\hat{\boldsymbol{e}}^{\mathrm{H}} \cdot \hat{\boldsymbol{j}}\| \leqslant \|\hat{\boldsymbol{e}}\|\|\hat{\boldsymbol{j}}\|$. This gives

$$\eta\varepsilon_{\inf}\|\hat{\boldsymbol{e}}\|^2 \leqslant \|\hat{\boldsymbol{e}}\|\|\hat{\boldsymbol{j}}\| \qquad \text{or equivalently} \qquad \|\hat{\boldsymbol{e}}\| \leqslant \frac{\|\hat{\boldsymbol{j}}\|}{\eta\varepsilon_{\inf}} \tag{4.13}$$

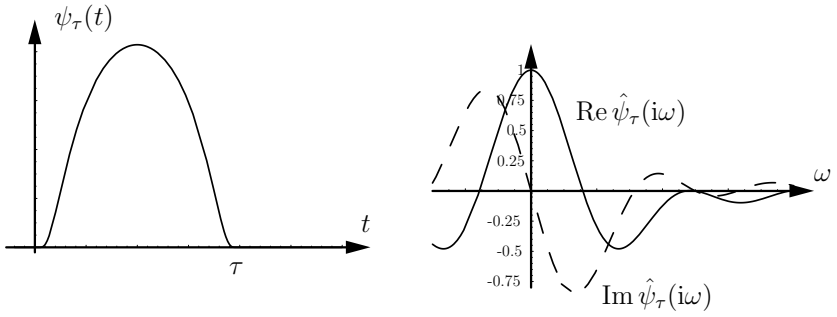

Figure 4. Example of the mollifier used in the definition of the smoothed fields (4.17) and (4.18).

where $\|\cdot\|$ denotes the L^2-norm in $\mathbb{R}^3$, i.e. $\|\hat{\boldsymbol{\jmath}}\| = \int_{\mathbb{R}^3} |\hat{\boldsymbol{\jmath}}(\boldsymbol{x})|^2 \,\mathrm{d}V$. The above estimate is repeated for the error equation (4.10). In this estimate the source term is given by $s(\varepsilon - \varepsilon')\hat{\boldsymbol{e}}$. The error $\hat{\boldsymbol{e}}' - \hat{\boldsymbol{e}}$ is estimated as

$$\|\hat{\boldsymbol{e}}' - \hat{\boldsymbol{e}}\| \leqslant \frac{\|s(\varepsilon' - \varepsilon)\hat{\boldsymbol{e}}\|}{\eta \varepsilon'_{\mathrm{inf}}} \tag{4.14}$$

where $\varepsilon'_{\mathrm{inf}} = \inf_{\boldsymbol{x}\in\mathbb{R}^3} \inf_{|\boldsymbol{u}|=1} \boldsymbol{u}^{\mathrm{H}} \cdot \varepsilon'_\infty \boldsymbol{u}$. The bound (4.13) on the original fields and the definition of the approximate constitutive map (4.1) on the constitutive map are used to get the estimate

$$\|\hat{\boldsymbol{e}}' - \hat{\boldsymbol{e}}\| \leqslant \frac{\|s(s^2 + \nu s)\| \, \|\hat{\boldsymbol{\jmath}}\|}{\left|s^2 + \nu s + w_0^2\right| \eta^2 \varepsilon_{\mathrm{inf}} \varepsilon'_{\mathrm{inf}}} \sup_{\boldsymbol{x}\in\mathbb{R}^3} |\varepsilon'_\infty - \varepsilon_\infty|. \tag{4.15}$$

This estimate shows that the Laplace-domain error fields approach zero for fixed values of the Laplace parameter s as the approximation constant ω_0 increases, i.e.

$$\|\hat{\boldsymbol{e}}'(\cdot, s) - \hat{\boldsymbol{e}}(\cdot, s)\| \to 0 \qquad \text{as} \quad \omega_0 \to \infty. \tag{4.16}$$

In general, the approximate fields do not approach the original fields in the time domain, due to the lack of approximation in the high-frequency part of the constitutive relations, i.e. the wave-front sets of the solutions do not agree. However, the approximation was only designed to be valid in the frequency range $[\omega_{\min}, \omega_{\max}]$. This frequency range is transformed to the time domain by a smoothing procedure. Introduce a set of smoothed fields as

$$\boldsymbol{e}_\tau(\boldsymbol{x}, t) = \int_0^t \boldsymbol{e}(\boldsymbol{x}, t - t')\psi_\tau(t') \,\mathrm{d}t' = (\boldsymbol{e} * \psi_\tau)(\boldsymbol{x}, t) \tag{4.17}$$

and similarly for the approximate fields $\boldsymbol{e}'_\tau$. The weight function $\psi_\tau(t) = \tau^{-1}\psi(t/\tau)$ is a smooth and positive function with unit integral that is supported in $[0, \tau]$, i.e. a mollifier, see figure 4. The smoothed fields have the Laplace-domain representation

$$\boldsymbol{e}_\tau(\boldsymbol{x}, t) = \frac{1}{2\pi} \int_{\mathbb{R}} \mathrm{e}^{(\eta + \mathrm{i}\omega)t} \hat{\boldsymbol{e}}(\boldsymbol{x}, \eta + \mathrm{i}\omega) \widehat{\psi}_\tau(\eta + \mathrm{i}\omega) \,\mathrm{d}\omega \qquad \text{for} \quad \eta \geqslant 0. \tag{4.18}$$

The Laplace transformed version of the weight function $\widehat{\psi}(s)$ is analytic for $\mathrm{Re}\, s > s_0 > -\infty$ and decays faster than every polynomial in s, i.e. there are numbers C_M such that

$$|\widehat{\psi}_\tau(s)| \leqslant C_M(1 + |\tau s|)^{-M} \qquad \text{for} \quad s \in \mathbb{C}_+, \quad \tau > 0 \quad \text{and} \quad M = 0, 1, \ldots. \tag{4.19}$$

Observe that the weight function approaches the Dirac delta distribution $\delta(t)$ for small times τ, i.e. $\psi_\tau(t) \to \delta(t)$ as $\tau \to 0$, and hence the frequency filtered fields resemble the original fields for small values of τ if the fields are sufficiently smooth. The smoothing time τ is obviously

related to the frequency band $[\omega_{\min}, \omega_{\max}]$ of the problem. With an averaging of N mollifiers per wavelength, the smoothing time is $\tau \approx 2\pi\omega_{\max}^{-1}N^{-1}$. In the numerical example in section 6, we use $N = 15$.

We use the above estimates to show convergence of the constitutive approximation in the time domain, i.e.

$$\int_0^T \int_{\mathbb{R}^3} |\boldsymbol{e}'_\tau(\boldsymbol{x}, t) - \boldsymbol{e}_\tau(\boldsymbol{x}, t)|^2 \,\mathrm{d}V \,\mathrm{d}t \to 0 \qquad \text{as} \quad \omega_0 \to \infty \tag{4.20}$$

for fixed τ and T. In fact, the integral is estimated as

$$\begin{aligned}\int_0^T \mathrm{e}^{2\eta t}\,\mathrm{e}^{-2\eta t}\|\boldsymbol{e}'_\tau(\cdot, t) - \boldsymbol{e}_\tau(\cdot, t)\|^2 \,\mathrm{d}t &\leqslant \mathrm{e}^{2\eta T}\int_0^\infty \mathrm{e}^{-2\eta t}\|\boldsymbol{e}'_\tau(\cdot, t) - \boldsymbol{e}_\tau(\cdot, t)\|^2 \,\mathrm{d}t \\ &= \frac{2\mathrm{e}^{\eta}t}{2\pi}\int_{\mathbb{R}} \|\hat{\boldsymbol{e}}'(\cdot, \eta + \mathrm{i}\omega) - \hat{\boldsymbol{e}}(\cdot, \eta + \mathrm{i}\omega)\|^2 |\widehat{\psi}_\tau(\eta + \mathrm{i}\omega)|^2 \,\mathrm{d}\omega \\ &\leqslant \left(\frac{CC_M\,\mathrm{e}^{\eta T}}{\nu\omega_0^2\eta^2\varepsilon_{\inf}\varepsilon'_{\inf}\tau^{3/2}} \sup_{\omega\in\mathbb{R}} \|\hat{\boldsymbol{\jmath}}(\cdot, \eta + \mathrm{i}\omega)\| \sup_{\boldsymbol{x}\in\mathbb{R}^3} |\varepsilon'_\infty - \varepsilon_\infty|\right)^2. \end{aligned} \tag{4.21}$$

The first inequality is trivial, the second step is the Parseval relation [2]. The final step is based on estimate (4.15) together with the supremum-type estimate

$$\begin{aligned}&\int_{\mathbb{R}} \left|\frac{s(s^2 + \nu s)C_M}{\left(s^2 + \nu s + \omega_0^2\right)(1 + |\tau s|)^M}\right|^2_{s=\eta+\mathrm{i}\omega} \mathrm{d}\omega \\ &\qquad \leqslant \frac{C_M^2}{\inf_{\omega\in\mathbb{R}}\left|s^2 + \nu s + \omega_0^2\right|^2_{s=\eta+\mathrm{i}\omega}} \int_{\mathbb{R}} \left|\frac{s(s^2 + \nu s)}{(1 + |\tau s|)^M}\right|^2_{s=\eta+\mathrm{i}\omega} \mathrm{d}\omega \leqslant \left(\frac{C_M C}{\nu\omega_0^2\tau^{3/2}}\right)^2\end{aligned}$$

where the M in (4.19) is such that $M \geqslant 4$ and the constant C only depends on ν and M. The estimate (4.21) is valid for all $\eta > 0$ and all $T \geqslant 0$. The choice $\eta = 2/T$ eliminates the exponential growth rate in estimate (4.21). This gives the time-domain convergence estimate

$$\left(\int_0^T \|\boldsymbol{e}'_\tau(\cdot, t) - \boldsymbol{e}_\tau(\cdot, t)\|^2 \,\mathrm{d}t\right)^{1/2} \leqslant \frac{C_4 C\,\mathrm{e}^2 T^2}{4\nu\omega_0^2\varepsilon_{\inf}\varepsilon'_{\inf}\tau^{3/2}} \sup_{\omega\in\mathbb{R}} \|\hat{\boldsymbol{\jmath}}(\cdot, \mathrm{i}\omega)\| \sup_{\boldsymbol{x}\in\mathbb{R}^3} |\varepsilon_\infty - \varepsilon'_\infty|. \tag{4.22}$$

This shows that the approximate solution approaches the original solution for all bounded times T and all fixed smoothing times τ as the approximation parameter ω_0 increases to infinity.

4.3. Frequency-domain convergence

The estimate (4.22) deteriorates as $T \to \infty$ and it is not possible to use a classical inverse Fourier transform to obtain frequency-domain estimates. However, the growth rate $\mathrm{O}(T^2)$ is not severe and the theory of temperate distributions [29] can be used to get a weak frequency-domain convergence. Estimate (4.13) and an analogous estimate for the approximate fields together with a similar estimate as (4.21) show that $\boldsymbol{e}_\tau(\boldsymbol{x}, t)$ and $\boldsymbol{e}'_\tau(\boldsymbol{x}, t)$ are tempered distributions. The approximate fields $\boldsymbol{e}'_\tau(\boldsymbol{x}, t)$ converge to the original fields $\boldsymbol{e}_\tau(\boldsymbol{x}, t)$ in the sense of distributions, i.e.

$$\int_0^\infty \int_{\mathbb{R}^3} |\boldsymbol{e}'_\tau(\boldsymbol{x}, t) - \boldsymbol{e}_\tau(\boldsymbol{x}, t)|^2 \phi(t) \,\mathrm{d}V \,\mathrm{d}t \to 0 \qquad \text{as} \quad \omega_0 \to \infty \quad \text{for all} \quad \phi \in \mathcal{S}. \tag{4.23}$$

The Schwartz class $\mathcal{S}$ consists of all functions $\phi(\omega)$ such that $\sup_{\omega\in\mathbb{R}}\left|\omega^\alpha \partial_\omega^\beta f(\omega)\right| < \infty$ for all α and β. The Fourier transform is well defined for tempered distributions and hence the

approximate fields converge to the original fields in the frequency domain in the sense of distributions, i.e.

$$\int_{\mathbb{R}}\int_{\mathbb{R}^3} |\hat{\boldsymbol{e}}'_\tau(\boldsymbol{x}, \mathrm{i}\omega) - \hat{\boldsymbol{e}}_\tau(\boldsymbol{x}, \mathrm{i}\omega)|^2 \phi(\omega)\,\mathrm{d}V\,\mathrm{d}\omega \to 0 \qquad \text{as} \quad \omega_0 \to \infty \quad \text{for all} \quad \phi \in \mathcal{S}. \tag{4.24}$$

Observe that estimate (4.22) is not sharp. In many cases, it is possible to show that the fields decay as time evolves, e.g., if the current is compactly supported both in time and space, a time-domain estimate gives $\|\boldsymbol{e}_\tau(\cdot, T)\| = \mathrm{O}(1)$ as $T \to \infty$. Moreover, if the fields radiate in $\mathbb{R}^3$, it has been shown that the energy of non-static fields in any bounded region decays as $T \to \infty$, see [3]. Also observe that a similar convergence estimate holds for the approximate fields in the case of sufficiently smooth currents, e.g., if $\|\hat{\boldsymbol{j}}(\cdot, s)\| = \mathrm{O}(|s|^{-4})$.

The construction above shows that it is possible to construct arbitrarily good approximations of a constitutive relation with a prescribed instantaneous response as long as the size of the instantaneous response decreases. The requirement to decrease the instantaneous response can be interpreted as a requirement to increase the wave-front speed. See also [18], where a similar construction is used for the acoustic wave equation.

5. Upper bound on the instantaneous response

In section 4, it was shown that it is possible to construct an approximate constitutive map such that the error of the corresponding approximate fields is small. In the construction (4.1), the instantaneous response decreased. In the isotropic case this corresponds to an increased wave-front speed and hence information is allowed to travel faster. The convergence for the approximate fields follows from the passivity of the approximate model. In this section, we discuss the possibility of constructing an approximate constitutive map such that the instantaneous response is increased. In the isotropic case, the wave-front speed of the approximate problem is hence decreased and so is the maximal speed of information. It is shown that in a passive approximation which is exact in a set of complex-valued frequencies the instantaneous response is bounded from above.

For the convergence estimate, it was essential that the constitutive maps were passive. To generalize the approximation in section 4, we consider an approximation based on Nevanlinna–Pick theory [1, 10], see also [16] for a general discussion about bounded analytical functions.

We start with a short review of the Nevanlinna–Pick theory. A function f is in the Nevanlinna class if $\mathrm{Re}\, f(s) \geqslant 0$ and $f(s)$ is analytic for $\mathrm{Re}\, s > 0$, i.e. $f : \mathbb{C}_+ \to \overline{\mathbb{C}}_+$. The Nevanlinna–Pick problem concerns the construction of a function f in the Nevanlinna class with prescribed values at a given set of points. For our purpose it is sufficient to consider the following version: construct a function f in the Nevanlinna class such that

$$f(s_i) = f_i \qquad \text{for} \quad i = 1, 2, \ldots n \tag{5.1}$$

where s_i and $f_i, i = 1, 2, \ldots, n$ are the given complex-valued numbers such that $\mathrm{Re}\, s_i > 0$ and $\mathrm{Re}\, f_i \geqslant 0$, respectively, see also figure 5. The interpolation problem is soluble if and only if the Nevanlinna matrix

$$\mathbf{N} = \left[\frac{f_i + f_j^*}{s_i + s_j^*}; i, j = 1, 2, \ldots, n \right] \tag{5.2}$$

is non-negative definite, see theorem 3.3.3 in [1]. Moreover, if the matrix is singular, the function $f(s)$ is unique and equal to a real-valued rational function.

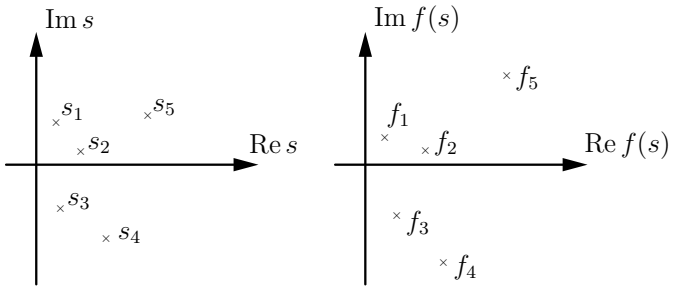

Figure 5. Example of the Nevanlinna–Pick interpolation problem. A function $f(s)$, analytic in $\mathbb{C}_+$, is constructed such that $f(s_i) = f_i$ and $\operatorname{Re} f(s) \geqslant 0$ for $s \in \mathbb{C}_+$.

The Nevanlinna–Pick theory can be used to construct an approximate constitutive map that is identical to the original map for the frequencies $s_i, i = 1, 2, \ldots, n$. The Nevanlinna–Pick theory ensures that the approximate map remains passive. We use the Nevanlinna–Pick problem to get some insight into the instantaneous response of the constitutive map. Let $\boldsymbol{\varepsilon}$ be a passive constitutive map, i.e. $\operatorname{Re} s\boldsymbol{\varepsilon}(s) \geqslant 0$. We construct an approximate passive constitutive map $\boldsymbol{\varepsilon}'$ such that

$$\boldsymbol{\varepsilon}'(s_i) = \boldsymbol{\varepsilon}(s_i) \qquad \text{for} \quad \operatorname{Re} s_i > 0 \quad i = 1, 2, \ldots, n. \tag{5.3}$$

For the construction of $\boldsymbol{\varepsilon}'$, we consider a set of functions $f_k(s)$ in the Nevanlinna class. The functions $f_k(s; \boldsymbol{u}_k), k = 1, 2, \ldots,$ are defined by

$$f_k(s; \boldsymbol{u}_k) = \boldsymbol{u}_k^{\mathrm{H}} \cdot s\boldsymbol{\varepsilon}(s)\boldsymbol{u}k \qquad \text{with} \quad \boldsymbol{u}_k \in \mathbb{C}^3 \times \mathbb{C}^3 \quad \text{and} \quad |\boldsymbol{u}_k| = 1. \tag{5.4}$$

These functions are in the Nevanlinna class and for sufficiently many column matrices $\boldsymbol{u}$ the map $\boldsymbol{\varepsilon}(s)$ is uniquely determined by the values of $f_k(s; \boldsymbol{u}_k)$, e.g.,

$$\boldsymbol{u}_1 = \begin{pmatrix} 1 \\ 0 \\ 0 \\ 0 \\ 0 \\ 0 \end{pmatrix} \qquad \boldsymbol{u}_2 = \begin{pmatrix} 0 \\ 1 \\ 0 \\ 0 \\ 0 \\ 0 \end{pmatrix} \qquad \boldsymbol{u}_3 = \frac{1}{\sqrt{2}} \begin{pmatrix} 1 \\ 1 \\ 0 \\ 0 \\ 0 \\ 0 \end{pmatrix} \qquad \text{and} \qquad \boldsymbol{u}_4 = \frac{1}{\sqrt{2}} \begin{pmatrix} 1 \\ \mathrm{i} \\ 0 \\ 0 \\ 0 \\ 0 \end{pmatrix} \tag{5.5}$$

determine the four elements $\epsilon_{1,1}, \epsilon_{2,2}, \epsilon_{1,2}$ and $\epsilon_{1,2}$. The general bi-anisotropic model is determined by 36 column matrices. Let us construct a constitutive map $\boldsymbol{\varepsilon}'(s)$ with the prescribed instantaneous response $\boldsymbol{\varepsilon}'_\infty$, i.e.

$$\lim_{s\to\infty} \boldsymbol{\varepsilon}'(s) = \boldsymbol{\varepsilon}'_\infty \qquad \text{and} \qquad \boldsymbol{\varepsilon}'(s_i) = \boldsymbol{\varepsilon}(s_i) \qquad \text{for} \quad i = 1, 2, \ldots, n \tag{5.6}$$

with $\operatorname{Re} s_i > 0$.

The Nevanlinna–Pick theory is used to show that the instantaneous response of the approximate constitutive map is bounded from above. To bound the approximate instantaneous response, we first observe that $\operatorname{Re}\{s\boldsymbol{\varepsilon}'(s) - s\boldsymbol{\varepsilon}'_\infty\} \geqslant 0$ for all $s \in \mathbb{C}_+$, see (2.10). Moreover, the Nevanlinna–Pick problem gives a necessary and sufficient condition for this inequality. From the interpolation (5.6), we get the following elements in the Nevanlinna matrix:

$$\begin{aligned} \mathbf{N}^{(k)}_{i,j} &= \frac{\boldsymbol{u}_k^{\mathrm{H}} \cdot (s_i\boldsymbol{\varepsilon}(s_i) - s_i\boldsymbol{\varepsilon}'_\infty)\boldsymbol{u}_k + \left(\boldsymbol{u}_k^{\mathrm{H}} \cdot (s_j\boldsymbol{\varepsilon}(s_j) - s_j\boldsymbol{\varepsilon}'_\infty)\boldsymbol{u}_k\right)^*}{s_i + s_j^*} \\ &= \frac{\boldsymbol{u}_k^{\mathrm{H}} \cdot s_i\boldsymbol{\varepsilon}(s_i)\boldsymbol{u}_k + \left(\boldsymbol{u}_k^{\mathrm{H}} \cdot s_j\boldsymbol{\varepsilon}(s_j)\boldsymbol{u}_k\right)^*}{s_i + s_j^*} - \boldsymbol{u}_k^{\mathrm{H}} \cdot \boldsymbol{\varepsilon}'_\infty\boldsymbol{u}_k \end{aligned}$$

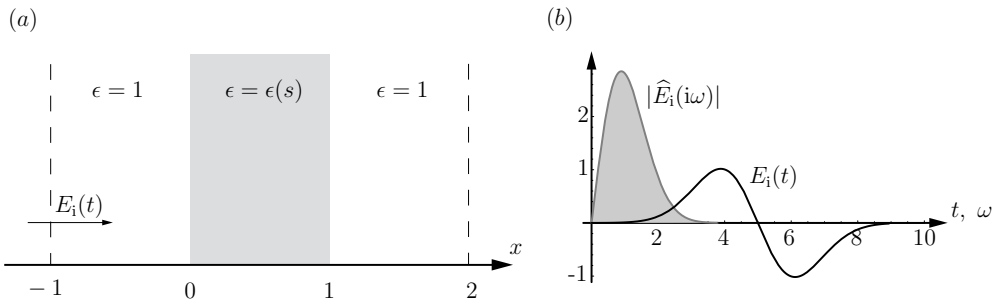

Figure 6. The slab geometry. (*a*) An electromagnetic field in vacuum impinges on a dielectric slab from the left. (*b*) The temporal and spectral behaviour of the incident field.

for $i, j = 1, 2, \ldots, n$ where the requirement $\operatorname{Im} \varepsilon'_\infty = 0$ is used. To satisfy the non-negative requirement we get an upper bound on the high-frequency response, i.e. $\mathbf{N}^{(k)} \geqslant 0$ implies

$$\boldsymbol{u}_k^{\mathrm{H}} \cdot \varepsilon'_\infty \boldsymbol{u}_k \leqslant \inf_{y_i \in \mathbb{C}} \frac{1}{\left|\sum_{i=1}^n y_i\right|^2} \sum_{i,j=1}^n y_i^* \frac{\boldsymbol{u}_k^{\mathrm{H}} \cdot s_i \varepsilon(s_i) \boldsymbol{u}_k + \left(\boldsymbol{u}_k^{\mathrm{H}} \cdot s_j \varepsilon(s_j) \boldsymbol{u}_k\right)^*}{s_i + s_j^*} y_j. \tag{5.7}$$

From (5.7), we conclude that there is an upper bound on the approximate instantaneous response, i.e. it is not possible to find a passive constitutive map with an arbitrary large instantaneous response with prescribed values.

6. Numerical illustration of the non-unique instantaneous response

As a numerical example of the non-uniqueness of the instantaneous response, we consider a scattering problem in one spatial dimension. An incident plane wave E_{i} in free space impinges on an isotropic and dielectric slab, see figure 6(*a*). The slab is modelled by the Debye–Lorentz type model [19, 20]

$$\epsilon(s) = 2 + \frac{17}{7+s} + \frac{4}{s^2 + 0.5s + 4} + \frac{400}{s^2 + 4s + 13^2} \tag{6.1}$$

and the free-space region by $\epsilon = 1$. For notational simplicity, we let $\epsilon_0 = \mu_0 = 1$. The incident wave field is given by $E_{\mathrm{i}}(t) = 1.5(t-5)\,\mathrm{e}^{-0.4(t-5)^2}$ for $t \geqslant 0$ and $E_{\mathrm{i}}(t) = 0$ for $t < 0$. The amplitude spectrum of the wave field is essentially confined to the frequency range $[0, 4]$, see figure 6(*b*).

We consider two approximate models of the slab. The first approximate model is constructed in agreement with the procedure in section 4, i.e. we add a Lorentz state with a high resonance frequency and subtract the low-frequency value from the instantaneous response. With the resonance frequency ω_0, we get the first approximate constitutive map

$$\epsilon'(s) = \epsilon(s) + \frac{\omega_0^2}{s^2 + 2s + \omega_0^2} - 1. \tag{6.2}$$

This approximation is passive and the error is $\sup_{\omega \in [0,4]} |\epsilon'(\mathrm{i}\omega) - \epsilon(\mathrm{i}\omega)| = 0.07$ for $\omega_0 = 17$, see figure 7(*a*). The wave-front speed of the approximate model is higher then the original wave-front speed, i.e. $c'_\infty = \epsilon_\infty'^{-1/2} = 1 > c_\infty = \epsilon_\infty^{-1/2} = 2^{-1/2}$, see figure 7(*b*).

To illustrate the difficulties with active models, we consider a second approximation of the constitutive map. We construct the approximate constitutive map by subtraction of a

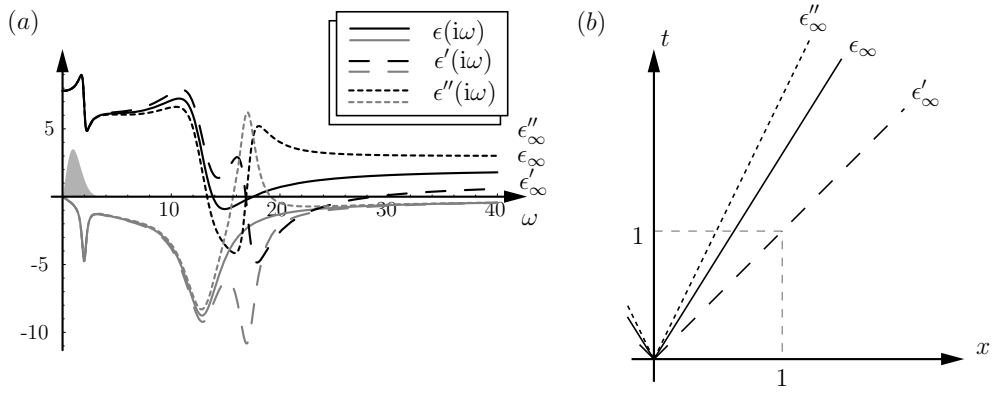

Figure 7. The permittivity profiles of (6.1), (6.2) and (6.3) with $\omega_0 = 17$. (*a*) The real- and imaginary-valued parts of the permittivity are given by the black and grey curves, respectively. Observe that the imaginary-valued part of (6.3) is positive, the medium is active, for a band of frequencies around $\omega = 17$. The frequency spectra of the incident pulse is illustrated by the shaded pulse. Observe that the pulse is essentially confined to the frequencies $|\omega| < 4$, see figure 6(*b*). (*b*) The wave-front characteristics of the different models. The wave-front speed of the first and second approximations is higher and lower than the wave-front speed of the original approximation, respectively.

high-frequency Lorentz state and addition of the low-frequency value to the instantaneous response, i.e.

$$\epsilon''(s) = \epsilon(s) - \frac{\omega^2}{s^2 + 2s + \omega^2} + 1 \tag{6.3}$$

see figure 7(*a*). The error of this second approximation is identical to the error of the first approximation. However, the second approximation is not passive, i.e. there are $s \in \mathbb{C}_+$ such that $\mathrm{Re}\, s\epsilon''(s) < 0$. Moreover, the wave-front speed of the second approximation is lower then the wave-front speed of the first approximation, i.e. $c''_\infty = 3^{-1/2} < c_\infty = 2^{-1/2}$, see figure 7(*b*).

We use a finite-difference scheme (FDTD) to determine the fields. For a plane wave normally impinging on the slab, the Maxwell equations reduce to the equations

$$\epsilon_\infty \partial_t E + \partial_x H + \partial_t P_1 + \partial_t P_2 + \partial_t P_3 + \partial_t P_4 = 0 \qquad \text{and} \qquad \partial_t H + \partial_x E = 0. \tag{6.4}$$

The Debye state P_1, and the Lorentz states P_k, $k = 2, 3, 4$, are updated with the equations

$$\begin{aligned} &\partial_t P_1 + 7P_1 = 17E \qquad \partial_t^2 P_2 + \tfrac{1}{2}\partial_t P_2 + 2^2 P_2 = 4E \\ &\partial_t^2 P_3 + 4\partial_t P_3 + 13^3 P_3 = 400E \qquad \text{and} \qquad \partial_t^2 P_4 + 2\partial_t P_4 + \omega_0^2 P_4 = \alpha E \end{aligned} \tag{6.5}$$

respectively. The parameters ϵ_∞ and α are given by $\epsilon_\infty = 2, 1, 3$ and $\alpha = 0, \omega_0^2, -\omega_0^2$ for the original, first approximate, and second approximate fields, respectively. The initial values of the fields are quiescent, i.e. $E(x, 0) = H(x, 0) = P_1(x, 0) = P_k(x, 0) = \partial_t P_k(x, 0) = 0$ for $k = 2, 3, 4$. At the boundary, we use the right- and left-going wave constituents [19]

$$\frac{E(-1, t) + H(-1, t)}{2} = E_{\mathrm{i}}(t) \qquad \text{and} \qquad \frac{E(2, t) - H(2, t)}{2} = 0 \tag{6.6}$$

respectively. In the numerical solution, the Maxwell equations (6.4) and the state equations (6.5) were discretized by central differences on a equidistant grid, i.e. a leap-frog scheme was used [31]. The spatial region was discretized by 300 grid points, i.e. $\Delta x = 0.01$. The temporal step size was half of the spatial grid size $\Delta t = \Delta x/2$.

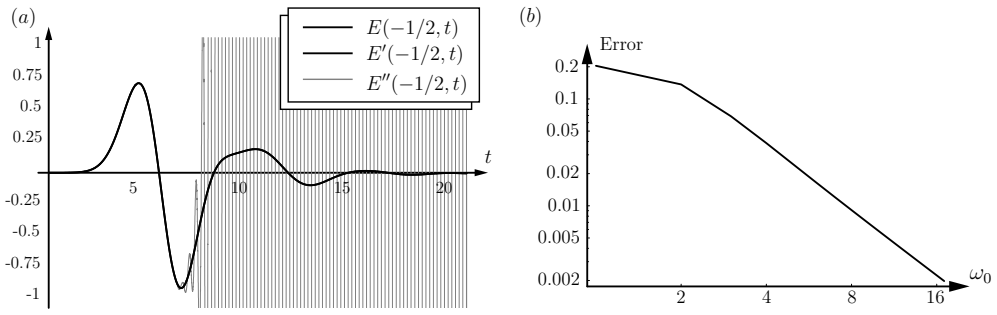

Figure 8. The scattered fields in the slab problem. (a) The electric fields at $x = -1/2$ for the constitutive maps (6.1), (6.2) and (6.3). The fields of the first approximation approximate the original fields well (the error is of the order 0.1% as seen in (b)) whereas the fields of the second approximation give a bad approximation due to the exponential growth rate of the fields. Observe that the field values are cut for values larger than 1 and, hence, the exponential growth rate of the second approximation E'' is not shown in the figure. (b) The error of the first approximation as a function of the resonance frequency ω_0. Observe that the error decays as ω_0^{-2} as predicted in (4.22).

The result of the simulation is depicted in figure 8. In figure 8(a), the original field E, the first approximate field E' and the second approximate field E'' are shown at the point $x = -1/2$ for the resonance frequency $\omega_0 = 17$. It is not possible to distinguish the first approximate field from the original field in the figure (the error is of the order 0.001). The second approximate field only approximates the original field for short times. As time evolves the amplitude of the second approximate field increases exponentially and so does the error of the approximation. The failure of the second approximation can be understood from the lack of passivity in this approximation. And since active (non-passive) medium models allow the field values to increase in time the approximation deteriorates. It is also interesting to compare the wave-front speed of the different approximate models. The wave-front speed, $c_\infty = \epsilon_\infty^{-1/2}$, is the speed of the wave-front set of the solution. It is also the maximal speed that the solution can propagate. Observe that the first approximate field has a higher wave-front speed than the wave-front speed of the original field whereas the wave-front speed of the second approximation is lower, see figure 7. The error of the first approximation is depicted in figure 8(b) as a function of the resonance frequency ω_0. The error decays as ω_0^{-2} as predicted in (4.22), see also (4.3).

Observe that wave fields are well resolved on the grid. The centre frequency of the incident wave field, $\omega = 2$, corresponds to the free-space wavelength $\lambda = \pi$. The highest Lorentz state has the resonance frequency $\omega_0 = 17$ with the equivalent wavelength 0.37. A second simulation with 3000 grid points was also performed to verify the numerical results. Observe that the fields depicted in figure 8 are not smoothed. The smoothed (4.17) fields with smoothing time $\tau = 2\pi/4/15 \approx 0.1$ have been computed and their graphs are not distinguishable from the graphs depicted in figure 8. In an attempt to eliminate the exponential growth of the second approximate fields a smoothing time $t = 1.0$ was tested. However, due to the exponential growth rate of the fields, the smoothing is not sufficient to eliminate the exponential growth rate.

7. Conclusions and discussion

In this paper, the uniqueness of the instantaneous response has been analysed. It has been shown that the instantaneous response is non-unique from a modelling point of view. The

constructed constitutive map is accurate in the region of interest. Outside this region, where the model is erroneous, the corresponding field values are bounded due to passivity.

Nevanlinna–Pick theory gives an upper bound on the size of the instantaneous response. It is interesting to compare this upper bound with the requirements from the special theory of relativity. In the special theory of relativity [20] the speed of electromagnetic waves in matter is bounded by the speed of electromagnetic waves in vacuum, i.e. the special theory of relativity predicts that it should be possible to bound the instantaneous response from below with the vacuum response. Physical arguments are also often used to conclude that the instantaneous response reduces to the vacuum response in the high-frequency limit [25].

A generalization of the analysis to nonlinear medium models is presently being considered.

Acknowledgments

I would like to acknowledge the valuable discussions with Gerhard Kristensson and Daniel Sjöberg. The partial support of the Swedish Research Council for Engineering Sciences is also gratefully acknowledged.

References

[1] Akhiezer N I 1965 *The Classical Moment Problem* (Edinburgh: Oliver and Boyd)
[2] Arfken G 1985 *Mathematical Methods for Physicists* 3rd edn (Orlando, FL: Academic)
[3] Ávila G S S and Costa D G 1980 Asymptotic properties of general symmetric hyperbolic systems *J. Funct. Phys.* **35** 49–63
[4] Balanis C A 1989 *Advanced Engineering Electromagnetics* (New York: Wiley)
[5] Bloom F 1981 *Ill-Posed Problems for Integrodifferential Equations in Mechanics and Electromagnetic* (Philadelphia, PA: SIAM)
[6] Born M and Wolf E 1980 *Principles of Optics* (Oxford: Pergamon)
[7] Brokate M and Sprekels J 1996 *Hysteresis and Phase Transitions* (Berlin: Springer)
[8] de Hoop A T 1995 *Handbook of Radiation and Scattering of Waves* (San Diego, CA: Academic)
[9] deGroot S R 1969 *The Maxwell Equations* (Amsterdam: North-Holland)
[10] Delsarte P, Genin Y and Kamp Y 1981 On the role of the Nevanlinna–Pick problem in circuit and system theory *Circuit Theory Appl.* **9** 177–87
[11] Eringen A C and Maugin G A 1990 *Electrodynamics of Continua I* (New York: Springer)
[12] Eringen A C and Maugin G A 1990 *Electrodynamics of Continua II* (New York: Springer)
[13] Evans L C 1998 *Partial Differential Equations* (Providence, RI: American Mathematical Society)
[14] Feynman R P, Leighton R B and Sands M 1965 *The Feynman Lectures on Physics* (Reading, MA: Addison-Wesley)
[15] Fridén J, Kristensson G and Sihvola A 1997 Effect of dissipation on the constitutive relations of bi-anisotropic media—the optical response *Electromagnetics* **17** 251–67
[16] Garnett J B 1981 *Bounded Analytic Functions* (New York: Academic)
[17] Greene R E and Krantz S G 1997 *Function Theory of One Complex Variable* (New York: Wiley)
[18] Gustafsson M 2000 The Bremmer series for a multi-dimensional acoustic scattering problem *J. Phys. A: Math. Gen.* **33** 1921–32
[19] Gustafsson M 2000 Wave splitting in direct and inverse scattering problems *PhD Thesis* Lund Institute of Technology, Department of Electromagnetic Theory, Lund, Sweden webpage http://www.es.lth.se/home/mats
[20] Jackson J D 1999 *Classical Electrodynamics* 3rd edn (New York: Wiley)
[21] Karlsson A and Kristensson G 1992 Constitutive relations, dissipation and reciprocity for the Maxwell equations in the time domain *J. Electromagn. Waves Appl.* **6** 537–51
[22] Kittel C 1986 *Introduction to Solid State Physics* 6th edn (New York: Wiley)
[23] Kong J A 1986 *Electromagnetic Wave Theory* (New York: Wiley)
[24] Kreiss H-O and Lorenz J 1989 *Initial-Boundary Value Problems and the Navier–Stokes Equations* (San Diego, CA: Academic)

[25] Landau L D, Lifshitz E M and Pitaevskiĭ L P 1984 *Electrodynamics of Continuous Media* 2nd edn (Oxford: Pergamon)
[26] Lindell I V, Sihvola A H and Suchy K 1995 Six-vector formalism in electromagnetics of bi-anisotropic media *J. Electromagn. Waves Appl.* **9** 887–903
[27] Lindell I V, Sihvola A H, Tretyakov S A and Viitanen A J 1994 *Electromagnetic Waves in Chiral and Bi-isotropic Media* (Boston, MA: Artech House)
[28] Post E J 1962 *Formal Structure of Electromagnetics* (Amsterdam: North-Holland)
[29] Richtmyer R D 1978 *Principles of Advanced Mathematical Physics* vol 1 (New York: Springer)
[30] Roberts T and Petropoulos P 1996 Asymptotics and energy estimates for electromagnetic pulses in dispersive media *J. Opt. Soc. Am.* A **13** 1204–17
[31] Strikwerda J C 1989 *Finite Difference Schemes and Partial Differential Equations* (New York: Chapman & Hall)
[32] Taflove A 1995 *Computational Electrodynamics: The Finite-Difference Time-Domain Method* (Boston, MA: Artech House)
[33] von Hippel A 1954 *Dielectric Materials and Applications* (Boston, MA: Artech House)
[34] Weinberg S 1995 *The Quantum Theory of Fields: Foundations* (Cambridge: Cambridge University Press)